International Journal of Mechanical Engineering and Technology (IJMET)
Volume 10, Issue 01, January 2019, pp. 107–118, Article ID: IJMET_10_01_011
Available online at http://www.iaeme.com/ijmet/issues.asp?JType=IJMET&VType=10&IType=1
ISSN Print: 0976-6340 and ISSN Online: 0976-6359

MODELING AND OPTIMIZATION OF BRAZING FOR AA 6061/ AISI 304LUSING GREY RELATIONAL ANALYSIS

Ahmed O. Al- Roubaiy, Saad Hameed Al-Shafaie, Wurood Asaad M.
College of Materials Engineering, Babylon University

ABSTRACT

In this paper, joining of aluminum alloy 6061 as annealed and austenitic stainless steel AISI 304L was carried out by furnace brazing at (620℃) and under protection of argon gas. Lap joints of AA 6061/AISI 304L were investigated with AlSi12, and AlSi10Cu4 filler alloys in form of paste using different brazing times (5, 10, 15, and 20 min). The optimum shear strength of the joint reached to (3.36 KN) at (10 min) using AlSi12 filler alloy. While, the maximum shear strength of the joint with AlSi10Cu4 filler alloy reached to (2.59 KN) at (15 min). In addition, microhardness of the interfacial layer of the joint with filler AlSi10Cu4 was higher than the microhardness value of the interfacial layer of the joint with AlSi12 filler alloy at the same brazing conditions. For each filler, at brazing time (5 min), lap joints were weak with minimum shear strength. Finally, the corrosion behavior of brazing joints in 3.5% NaCl was studied to evaluate the rate of corrosion for brazing joints. The minimum corrosion rate is achieved (0.005209mpy) (1.68μA) by (10 min) using AlSi12 filler alloy. Grey relational analysis (GRA) based on Taguchi method was applied using two factors, brazing time (T) and filler type (F) with four levels. The results showed that the variation of brazing time is the most affective parameter on the shear force, corrosion rate, and microhardness of the interfacial reaction layer. While, the type of filler alloy is slightly affective on the output response. In addition, these results manifested that the Taguchi based grey relational approach improves the properties of the output response of the joined AA 6061 and AISI 304L.

Key words: AA6061, AISI 304L, Filler alloys, brazing, Taguchi method, GRA, Interfacial reaction layer, Corrosion rate.

Cite this Article: Ahmed O. Al- Roubaiy, Saad Hameed Al-Shafaie, Wurood Asaad M, Modeling and Optimization of Brazing for AA 6061/ AISI 304Lusing Grey Relational Analysis, *International Journal of Mechanical Engineering and Technology* 10(1), 2019, pp. 107–118.
http://www.iaeme.com/IJMET/issues.asp?JType=IJMET&VType=10&IType=1

1. INTRODUCTION

The need for joints of aluminum alloy and stainless steel has highly increased in a wide range of industrial applications due to weight reduction and energy saving. The difficulties of

dissimilar metals joining return into the high differences in thermophysical properties between them as well the easy formation of intermetallic compound at high temperature, which effects on the mechanical properties of the joints. L. Peng et al. [1]. reported that the brazing metal consists of δ(Al, Fe, Si), α-Al (Si) and Al of the joint AA1060/AISI 304 by vacuum brazing technology method using Al-Si filler alloy. J. Yang et al. [2] found that the interface between the braze seam and the stainless steel contains Fe_4Al_{13} IMC layer of the joint AA6061/AISI304 using filler alloy of Zn-15Al-xZr.

To achieve a highly qualified joint between aluminum and stainless steel, various welding processes were investigated. R. Qiu et al. [3] conducted resistance spot welding with a cover plate of AA5052 to austenitic stainless steel, where reaction products of the joint contain Fe_2Al_5 and $FeAl_3$. E. Taban et. al. [4] successfully joined aluminum alloy 6061 to AISI 1018 steel that was investigated with friction stir welding. Intermetallic compounds (IMC_s) appeared, including FeAl and Fe_2Al_5 in the interfacial reaction layer. C. Dharmendra et al. [5] suggested the laser welding- brazing process to join zinc coated steel (DP600) with aluminum alloy (AA6061) using filler wire Zn_{85}-Al_{15} and various thicknesses of IMC with a difference in heat input.

S. H. Al- shafaie and S. B. Al-ghazaly [6] investigated improving properties of output response (elongation, yield stress, and ultimate tensile strength) of welded Al 6061 and Al 7075 aluminum alloy by friction stir welding. K. D. Dwivedi and A. Srivastava [7] found that Taguchi′s parameters design approach allows for improving the quality for the joint stainless steel 304 and C-25 carbon steel using a metal inert gas welding. By Taguchi design, it was found that the wire feed rate is the first parameter that has the highest effect on the hardness then current and voltage parameters.

In this paper, a Taguchi method is applied to conduct the experiments and a Grey Relational Analysis approach is used for development of a second–order polynomial model and optimize of corrosion rate, shear force and hardness of layer with the time and filler as input parameters.

2. EXPERIMENTAL WORK

AA 6061 and AISI 304L sheets with dimensions (60x18x1mm) are chosen to produce dissimilar joints by the brazing process. Two filler alloys AlSi12 and AlSi10Cu4 are applied as a paste form. The chemical compositions of base alloys and filler alloys are listed in Table1.

Table 1 Chemical composition of alloys (wt %) [8][9][10]

Alloy %	C	Cr	Si	Mn	P	Mo	Ni	Al	Cu	Fe	Mg	Ti	Zn
AISI304L	0.025	18.93	0.41	1.42	0.055	0.053	7.85	<0.001	0.164	Bal	-	-	-
AISI304L (Standard)[8]	≤ 0.03	18-20	≤ 1.00	≤ 2.00	≤ 0.045	-	8-11	-	-	Bal			
AA6061	-	0.11	0.91	0.23	-	-	0.06	96.78	0.14	0.57	0.99	0.12	0.08
AA 6061 (Standard)[9]		0.04-0.35	0.4-0.8	0.15%				96	0.15-0.4	0.7	0.8-1.2	0.15	0.25
AlSi12	-	-	11.9	0.01	-	-	-	Bal.	<0.01	o.14	0.01	<0.01	<0.01
AlSi12 Standard[10]			11-13	0.15				Bal.	0.30	0.8	0.01	0.20	0.2
AlSi10Cu4	-	-	10	0.02	-	-	-	Bal.	4	0.7	0.02	0.03	0.05
AlSi10Cu4 Standard[10]			9.3-10.7	0.15				Bal.	3.3-4.7	0.8	0.01	0.1-0.2	0.20

Before brazing, the workpieces were cleaned by silicon carbide abrasive paper and acetone to remove grease or oil. Then, all joints were fixed using a simple fixture of stainless steel to hold the assembly the pieces as shown Fig. (1). The pieces were produced by furnace using quartz tube in an argon atmosphere at rate 5 L/min. After the samples preparation was finished, samples with added fillers were heated to 620 ℃ for a variable holding times and finally cooled by furnace.

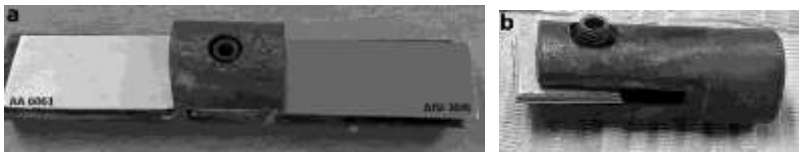

Figure 1 Fixtures for the joints: (a) for a lap joint: (b) for a small joint.

Based on initial experiments, the independent factors affecting the responses were identified as: holding time (T) and filler type (F) therefore, the influenced factors and their levels are tabulated in Table 2.

Table 2 Process parameters and their levels.

parameters	Unit	Coded/Actual level			
		1	2	3	4
Holding time (T)	min.	5	10	15	20
Filler type (F)	-	$AlSi_{12}$	$AlSi_{10}Cu_4$	----	----

After brazing, a typical cross- section of the joint was cut and mounted in self –setting epoxy resin. Then, course grinding was conducted on the mounted samples starting with sandpaper up to 2000. After that, polishing was done using diamond solution (0.1-0.3 micron) for (15 min) and etched with Keller's reagent ($5HNO_3$, 3HCl, 2HF, 200H2O) for 5-7 sec.

The distribution of the microhardness along the cross section of the joint was obtained by Vickers-microhardness test. Tensile shear test was applied for a joint with (102 mm) in length. Finally, Tafel test was applied for each joint to determine the current density and corrosion rate in NaCl solution with different brazing conditions.

3. RESULT AND DISCUSSION

The selected design metrics according to a Taguchi design orthogonal array (OA) are shown in Table 3. It was the two factor different levels containing 8 sets of actual conditions run which allowed the assessment of the effects the factors on the Corrosion Rate (CR), Shear Force (F_S), and Hardness of layer (HoL). The value of the output is organized in Table 3.

Table 3 Observed values for performance characteristics.

Exp. No	T	F	CR mpy	F_S KN	HoL HV
1	1	1	0.0190400	0.9186	98.70
2	1	2	0.0187800	0.8574	113.30
3	2	1	0.0052090	3.3600	262.40
4	2	2	0.0056103	2.2000	297.10
5	3	1	0.0103200	3.0700	360.10
6	3	2	0.0123780	2.5902	372.50
7	4	1	0.0143890	2.3992	393.25
8	4	2	0.0154480	2.0464	401.10

3.1. Parametric Analysis of Responses

Parametric analysis of each variable on CR, F_S and HoL are shown in Fig. 2. It is seen that as T increases above 5 min the CR of the joint decreases until 10 min, after that the CR of the joint increases. The minimum CR is achieved (0.005209mpy) (1.68μA) by (10 min) due to consider the suitable time to make a good wetting of the filler alloy at the substrate surface by the capillary reaction. That assists to produce a good joint with the fewest defects and less thickness of interfacial layer with phases a good corrosion resistance ($AlNi_3$) see fig 3.

While, the T increase to (15, 20 min) led to raise the corrosion resistance rate to (0.01032 and 0.014389 mpy) (3.33 μA, 4.64μA), respectively. This increasing of corrosion rate is due to the change in the microstructure of the interfacial joint; crack appearance and thickness growth of the interfacial layer which contains (IMC_s) see fig. 4.

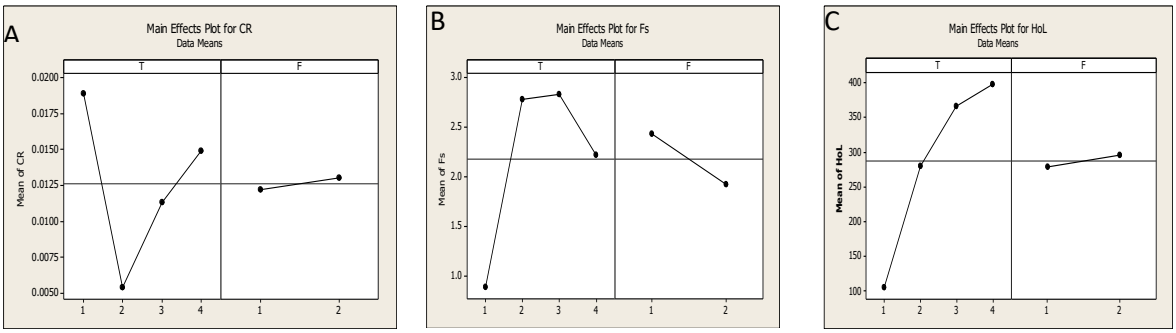

Figure 2 Main Effect Plots for A: CR, B: Fs and C: HoL.

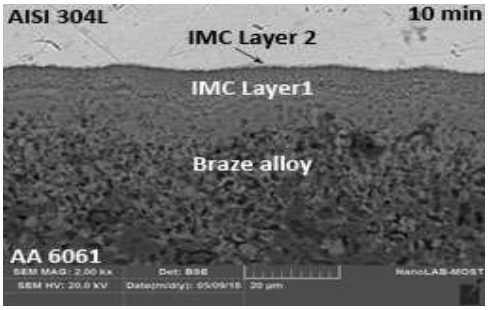

Figure 3 Microstructure of AA 6061/AISI 304L

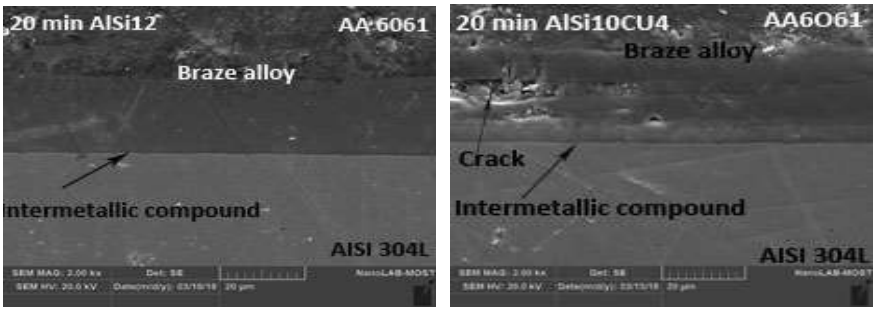

Figure 4 Microstructure for the joint with different filler alloys at different times

In addition, with 5 min T, for both filler alloys AlSi12 and AlSi10Cu4, the CR raised to (0.01904 mpy) (6.14 μA) and (0.01878 mpy) (11.52 μA) due to the brazing lack time that isn't enough to wet on the substrate by the filler alloy. That leads to crack formation and porosity. These defects at the joint lead to a galvanic corrosion because of the variation in the concentration of elements at the interfacial layer, see fig5 .

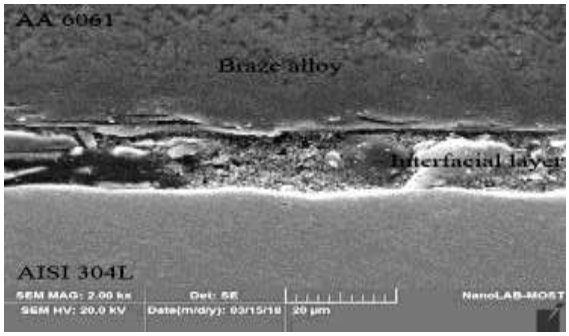

Figure 5 The microstructure for the interfacial joint at 5 min (SEM)

Type of the filler (F) affected on the rate of corrosion through using AlSi12 that improved the resistance of corrosion due to the presence of (4%Cu) in filler alloy that leads to the growth of the reaction layer [11].

In addition it is seen that as T increases above 5 min the Fs and HoL of brazing AA6061 and 304L increases. While as T increases above 10 min the Fs decreases but the HoL increases of the joint.

For both filler alloy, when the time of brazing joint increases above 10 min , the Fs of brazing joint AA6061/ 304L decreases due to the growth of the interfacial layer thickness, which consists of the intermetallic compounds, Roulin et. al. (1999) found the maximum of the shear strength joint is (21 MPa) after (10min) brazing time at the brazing temperature (600℃) during brazing of aluminum /stainless steel joints using eutectic brazing alloy Al-Si with different brazing times (5, 10, 20, 40, 60 min)by furnace process [12].

For each brazing time, the Fs of the joint tends to decrease with the filler alloy AlSi10Cu4 due to the 4%Cu in the filler alloy leads to the growth occurrence in the interfacial layer, this agreement with the present study, Dong et.al. (2012) obtained that the thickness of the interfacial layer for a joint with AlSi12 less than the thickness of it for the joint with AlSi10Cu4 [11], see fig. 6.

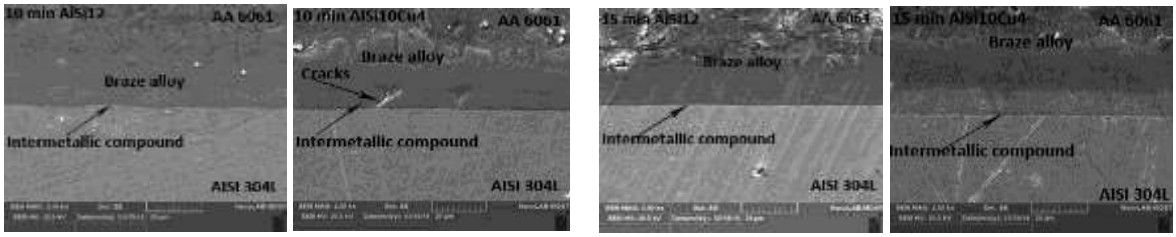

Figure 6 The effect of brazing time on the thickness of interfacial layer of the joint for both filler alloys (SEM)

For less than (10 min), at (5 min), the Fs value for the brazing joint reduced due to the lack of time that is required for a complete wetting between the braze alloy and the base alloy that led to the deboned of contact area between the faying surfaces.

When the time increases above 10 min, the average hardness of the interfacial layer increases due to the growth of the interfacial layer with IMC_s hardened layer by increasing the diffusion rate, see fig7.

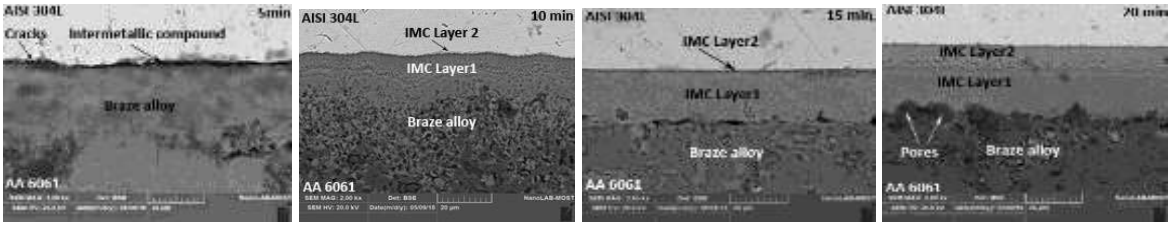

Figure 7 Microstructure of AA 6061/AISI 304L with the different brazing times (SEM) using AlSi12 filler alloy

At the brazing time (5 min), the hardness of the interfacial reaction of the joint is minimum due to the lack of time that is required for a complete wetting between the braze alloy and the base that led to to the occurrence deboned.

Besides that, the use of AlSi12 filler alloy led to a fall in the hardness compared with the using AlSi10Cu4 due to the presence Cu may be distributed in the grain boundaries to form Al_2Cu a brittle intermetallic compound [13,14].

Equations 1 -3 shown below are the predicted regression models for calculating output (corrosion rate, shear force and hardness of layer). Equations of output are developed with 95% confidence levels.

$$CR = 0.036376 - 0.022783\ T - 0.000589\ F + 0.004267\ T^2 + 0.000561\ T\times F \ldots\ldots\ldots \quad (1)$$

$$Fs = - 1.26032 + 3.55876\ T - 0.46480\ F - 0.62482\ T^2 - 0.01946\ T\times F \ldots\ldots\ldots \quad (2)$$

$$HoL = -173.344 + 280.984\ T + 28.025\ F - 35.719\ T^2 - 4.255\ T\times F \ldots\ldots\ldots \quad (3)$$

3.2. Checking the sufficiency of the model

The adequacy of the models so developed is then tested by using the analysis of variance technique (ANOVA). Using this technique, it can be noted that, as illustrated in Table 4, all the quadratic regression models significant ($0 < \text{p-value} < 0.05$), except F for all outputs (p-value > 0.05) and thus all the models adequately represent the experimental data.

Table 4 ANOVA Table for output.

Source	DF	Seq SS	Adj SS	Adj MS	F	P
For CR						
T	3	0.000197	0.000197	0.000066	134.34	0.001
F	1	0.000001	0.000001	0.000001	2.72	0.198
Residual Error	3	0.000001	0.000001	0.000000		
Total	7	0.000200				
For Fs						
T	3	4.9075	4.9075	1.6358	15.11	0.026
F	1	0.5273	0.5273	0.5273	4.87	0.114
Residual Error	3	0.3247	0.3247	0.1082		
Total	7	5.7595				
For HoL						
T	3	92174	92779	92174.4	43.82	0.001
F	1	605	605	604.7	0.29	0.615
Residual Error	3	10518	10518	2103.5		
Total	7	103297				

Another criterion that is commonly used to illustrate the adequacy of a predicted regression model is the coefficient of determination (R^2). For the models, the calculated R^2 values is 94.40%, 99.3% and 89.82 % for Cr, Fs and HoL respectively as shown in Table 5. These values indicate that the regression models are quite adequate. The validity of regression

models developed is further tested by drawing scatter diagrams. Typical scatter diagrams for all the models are presented in fig.8. The observed values and predicted values of the responses are scattered close to the 45° line, indicating an almost perfect fit of the developed empirical models.

Table 5 R^2 Test for CR, Fs and HoL regression model.

Response	**R^2 value**	**Remarks**
CR	94.40 %	Adequate
Fs	99.30 %	Adequate
HoL	89.82 %	Adequate

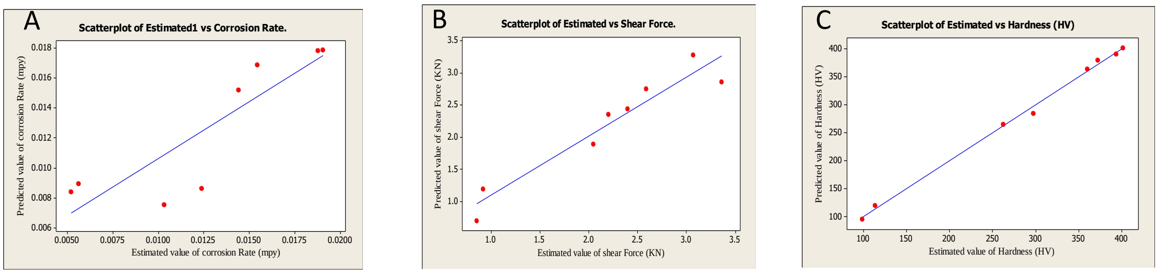

Figure 8 Scatter diagram of the A: CR, B: Fs and C: HoL.

3.3. Determination of Optimal Process Parameters in Grey Relation Analysis GRA

In this section, the use of the Taguchi design orthogonal array (OA) with the grey relation analysis (GRA) for determining the optimal process parameters is reported step by step.

3.3.1. Data Pre-Processing

In GRA, data pre-processing is required since the range and unit in one data sequence may differ from the others. Data pre-processing is also necessary when the sequence scatter range is too large, or when the directions of the target in the sequence are different. Data pre-processing is a process of transferring the original sequence to a comparable sequence. For this purpose, the experimental results are normalized in the range between zero and one. Depending on the characteristics of data sequence, there are various methodologies of data pre-processing available for the GRA.

Response or output can be converted into the comparative series $x_i^*(k)$ according to equations 4 to 6 for "the larger, the better", "the smaller, the better" and "values closer to the optimal value of response are better" characteristics respectively.

$$x_i^*(k) = \frac{X_i(k) - \max X_i(k)}{\max X_i(k) - \min X_i(k)} \quad \ldots \ldots \quad (4)$$

$$x_i^*(k) = \frac{\max X_i(k) - X_i(k)}{\max X_i(k) - \min X_i(k)} \quad \ldots \ldots \quad (5)$$

$$x_i^*(k) = \frac{|X_i(k) - X_{ob}(k)|}{\max X_i(k) - X_{ob}(k)} \quad \ldots \ldots \quad (6)$$

where, $x_i^*(k)$ and x_i (k) are the sequence after the data preprocessing and comparability sequence respectively, min x_i (k) is the smallest value of x_i (k) for the k^{th} response, and max X_i(k) is the largest value of X_i(k) for the k^{th} response, k=1 and 2 for corrosion rate, shear force and hardness of layer; i=1, 2, 3…, 8 for experiment numbers 1 to 8.

Table 6 shows the normalized results for corrosion rate, shear force and hardness of layer, where corrosion rate for the smaller the better, shear force for the larger the better, and hardness of layer for values closer to the optimal value of response are better.

All the sequences of each performance characteristic after data preprocessing using Equation 4-6 are presented in Table 6.

Table 6 The sequences of each performance characteristic after data processing.

Exp. No	CR	Fs	HoL
Reference sequence	1.000000	1.000000	1.000000
1	0.000000	0.024455	1.657290
2	0.018798	0.000000	1.529000
3	1.000000	1.000000	0.218800
4	0.970985	0.536482	0.086116
5	0.630468	0.884121	0.639719
6	0.481672	0.692400	0.748682
7	0.336274	0.616079	0.931019
8	0.259706	0.475106	1.000000

Now, $\Delta_{0i}(k)$ is the deviation sequence of the reference sequence $x_0^*(k)$and the comparability sequence $x_i^*(k)$., i.e.

$$\Delta_{0i}(k) = |X_0^*(k) - X_i^*(k)| \dots\dots\dots\dots\dots\dots\dots\dots\dots\dots\dots\dots (7)$$

Using Eq. 7 the deviation sequence Δ_{0i} can be computed and the results are clear in Table 7.

Table 7 The deviation sequences

Deviation sequences	Δ_{0i} (1)	Δ_{0i} (2)	Δ_{0i} (3)
Expt. No. 01	1.000000	0.975545	0.657290
Expt. No. 02	0.981202	1.000000	0.529000
Expt. No. 03	0.000000	0.000000	0.781200
Expt. No. 04	0.029015	0.463518	0.913884
Expt. No. 05	0.369532	0.115879	0.360281
Expt. No. 06	0.518328	0.307600	0.251318
Expt. No. 07	0.663726	0.383921	0.068981
Expt. No. 08	0.740294	0.524894	0.000000

3.3.2. The Grey Relational Coefficient and the Grey Relational Grade

After data pre-processing is performed, GRC is computed from the normalized data to establish a relationship between the preferred and actual data. The GRC is known as follows:

$$\xi_i(k) = \frac{\Delta_{min.} + \xi\Delta_{max.}}{\Delta_{0i}(k) + \xi\Delta_{max.}} \dots\dots\dots\dots\dots\dots\dots\dots\dots\dots\dots\dots (8)$$

The distinguishing or identification coefficient ,ξ, has been used to compensate for the effect of the data series and is defined between zero to one. The value of ξ has been taken equal to 0.5. The GRC for each experiment OA is shown in Table 8.

Table 8 Grey relational grade and its order in the optimization. After get the GRC, the GRG is calculated by averaging the GRC corresponding to every response. The overall evaluation of the multiple responses (output) is based on the GRG, that is:

$$\gamma_i = \frac{1}{n}\sum_{k=1}^{n} \xi_i(k) \ldots\ldots\ldots\ldots\ldots\ldots\ldots\ldots\ldots\ldots\ldots\ldots\ldots \quad (9)$$

Where γ_i the GRG for the i^{th} experiment and n is the number of output or responses. Table 8 shows the grey relational grade for each experiment using L8 OA. The higher grey relational grade represents that the corresponding experimental result is closer to the ideally normalized value. Experiment 3 has the best multiple performance characteristics among eight experiments because it has the highest grey relational grade. It can be seen that in the present study, the optimization of the complicated multiple performance characteristics of brazing of AISI 304L and AA 6061 has been converted into optimization of a grey relational grade.

Since the experimental design is orthogonal, it is then possible to separate out the effect of each process parameter on the grey relational grade at different levels. For example, the mean of the grey relational grade for the time at levels 1 and 2 can be calculated by averaging the grey relational grade for the experiments (1 and 2) and (3 and 4) and (5 and 6) and (7 and 8) respectively as shown in Table 8.

Table 8 Response table for the grey relational grade.

Expt. No.	Grey relational coefficient			Grey relational grade $\gamma_i = \frac{1}{3}(\xi\, i\,(1) + \xi\, i\,(2) + \xi\, i\,(3))$	Rank
	ξ_i (1) CR	ξ_i (2) Fs	ξ_i (3) HoL		
01	0.338858	0.333333	0.410096	0.360762	8
02	0.333333	0.337564	0.463457	0.378118	7
03	1	1	0.369055	0.789685	1
04	0.518932	0.945153	0.333333	0.599139	5
05	0.811848	0.575022	0.55914	0.64867	2
06	0.619118	0.491001	0.645161	0.585093	6
07	0.565661	0.429654	0.868838	0.621384	4
08	0.487855	0.403130	1	0.630328	3

The mean of the grey relational grade for each level of the other process parameters, namely, filler can be computed in the same manner. The mean of the grey relational grade for each level of the process parameters is summarized and shown in Table 9. In addition, the total mean of the grey relational grade for the eight experiments is also calculated and presented in Table 9.

Table 9 Response table for the grey relational grade.

Symbol	Process parameters	Grey relational grade				Main effect (max-min)	Rank
		Level 1	Level 2	Level 3	Level 4		
A	T	0.36944	0.694412*	0.616882	0.625856	0.324972	1
B	F	0.605125*	0.54817	-----	-----	0.056955	2
		The total mean value of the grey relational grade γ_m= 0.576647 * Levels for optimum grey relational grade					

Fig.9 shows the grey relational grade obtained for different process parameters. The mean of grey relational grade for each parameter is shown by horizontal line. Basically, the larger the grey relation grade is, the closer will be the product quality to the ideal value. Thus, larger grey relational grade is desired for optimum performance. Therefore, the optimal parameters setting for lesser corrosion rate, better shear force and nominal hardness of layer are (A_2B_1) as

presented in Table 9. Optimal level of the process parameters is the level with the highest grey relational grade.

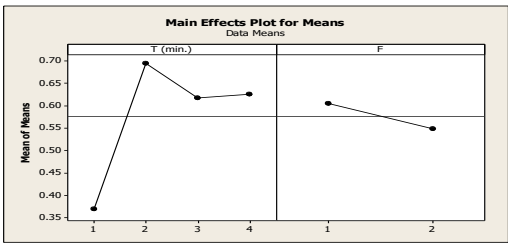

Figure 9 Effect of process parameters on the multi-performance characteristics.

Furthermore, ANOVA has been performed on grey relational grade to obtain contribution of each process parameter affecting the process characteristics jointly and is discussed in the forthcoming section.

3.3.3. Analysis of Variance for GRG

ANOVA for grey relational grade is presented in Table10. Percentage contributions for each term affecting grey relational grade are shown in fig.10. The figure clearly shows that time is the dominant parameter that affects grey relational grade and hence contributes in reducing corrosion rate improving shear force nominal hardness of layer.

Table 10: ANOVA of grey relational grade.

Source	DF	Seq SS	MS	F	Percentage contribution(ρ)
T	3	0.121687	0.040562	8.77	85.6631
F	1	0.006488	0.006488	1.40	4.567309
Error	3	0.013878	0.004626	-	9.769593
Total	7	0.142053		-	100.00000

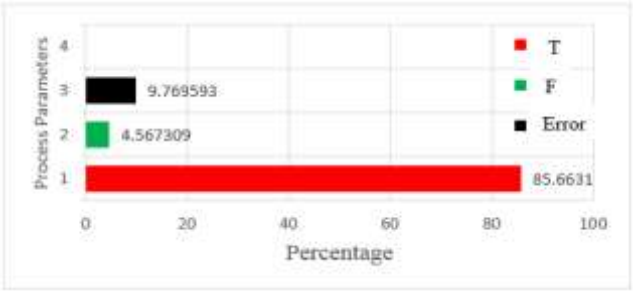

Figure 10 Percentage contributions of factors on the grey relational grade.

Based on the above discussion, the optimal process parameters are time at level 2, and filler at level 1 It can be seen from fig.10 that time is the most significant factor that affects the grey relational grade followed by filler.

3.3.4. Confirmation test

Confirmation test has been carried out to verify the improvement of performance characteristics in brazing of AA 6061/AISI 304L. The optimum parameters are selected for the confirmation test as presented in Table 11. The estimated grey relational grade $\hat{\gamma}$ using the optimal level of the process parameters can be calculated using following equation.

$$\hat{\gamma} = \gamma_m + \sum_{i=1}^{q} (\gamma_i - \gamma_m) \dots\dots\dots\dots\dots\dots\dots\dots\dots\dots\dots\dots\dots\dots (10)$$

where $\gamma_m$is the total mean of the grey relational grade γ_i is the mean of the grey relational grade at the optimal level, and q is the number of the process parameters that significantly affect multiple-performance characteristics.

The obtained process parameters, which give higher grey relational grade, are presented in Table 11. The predicted CR, Fs, HoL and GRG for the optimal process parameters are obtained using Equation 10 and also presented in Table 11 which shows the comparison of the experimental results using the initial (A_2B_1) and optimal (grey theory prediction design, A_2B_1) process parameters. Based on Table 11, the CR decreased from 0.0052090 to 0.0043070 mpy, Fs is accelerated from 3.3600 to 4.1400 KN and the HoL remain approximately constant at (262.40 ≈ 261.94) HV. The corresponding improvements in CR and Fs are 17.31%, 18.84 %, respectively. It is clearly shown that the multiple performance characteristics in the process are greatly improved through this study.

Table 11 Improvements in grey relational grade with optimized process parameters.

Condition description	**Optimal process parameters**	
	Initial process parameters	**Grey theory Prediction design**
Level	**A2B1**	**A2B1**
CR (mpy)	0.0043070	0.0052090
Fs (KN)	4.1400	3.3600
HoL (HV)	261.94	262.40
GRG	0.710672	0.789685
Improvement in grey relational grade = 0.079013		

4. CONCLUSIONS

- The shear force of the joint registered an optimum value 3.36KN with AlSi12 at 10 min. While the maximum shear force of the joint with AlSi10Cu4 reached to 2.59 KN at 15 min.
- For the lap joint at (10 min) using AlSi12, the minimum corrosion rate is 0.0052090 mpy.
- According to microhardness test, the interfacial layer of the joint with AlSi12 has less hardness than the hardness of the interfacial layer of joint using AlSi10Cu4.
- The optimum value for brazing time 10 min, filler alloy type AlSi12 respectively.
- The experiment exhibits the best factors combination and the predicted values were closer to the observed values.
- This approach easily converts the multiple performance characteristics into the GRG, thus simplifying the analysis.
- The results showed that the optimal condition based on the method can offer a better overall quality.

REFERENCES

[1] Peng Liu, Li Yajiang, Wang Juan, and Guo Jishi (2003) " Vacuum brazing technology and microstructure near the interface of Al/18-8 stainless steel", Materials Research Bulletin, pp.1493-1499.

[2] Yang Jinlong, Songbai Xue, Peng Xue, Zhaoping Lv, Weimin Long, Guanxing Zhang, Qingke Zhang, and Peng He (2016) " Development of Zn-15Al-xZr filler metals for Brazing 6061 aluminum alloy to stainless steel", Materials Science and Engineering A, pp. 425-434.

[3] Qiu Ranfeng, Chihiro Iwamoto, and Shinobu Satonaka (2008) " Interfacial microstructure and strength of steel/aluminum alloy joints welded by resistance spot welding with cover plate", Journal of Mterials Processing Technology, pp. 4186-4193.

[4] Taban Emel, Jerry E.Gould, and John C. Lippold (2010) " Dissimilar friction welding of 606-T6 aluminum and AISI1018 steel: Properties and microstructural characterization", Materials and Design, pp. 2305-2311.

[5] Dharmendra C., K.P.Rao, J.Wilden, S.Reich (2011) " Study on laser welding- brazing of Zinc coated steel aluminum alloy with a zinc based filler", Materials Science and Engineering A, 1497-1503.

[6] Saad Hameed Al-shafaie and Sara bahjet Al-ghazaly (2018) "Optimization of friction stir welding parameters of Al 6061 and Al 7075 using GRA",

[7] Kamaleshwar Dhar Dwivedi and Anurag Srivastava (2017) " Parametric Optimization of MIG Welding for Dissimilar Metals Using Taguchi Design Method" Department of Mechanical Engineering, S. R. Institute of Management and Technology, A. K. T. U. Lucknow, Inia, Volume 3.

[8] ASTM Handbook (1989) "Iron and metal products",vol. 01.01.

[9] ASM Handbook (1990) Properties and Selection: Nonferrous Alloys and Special-Purpose Materials, American society for Metals, Vol. 2.

[10] Lejeune Road (2007) Specification for Induction Brazing, American Welding Society (AWS), 2nd ed.

[11] Dong Honggang, Wenjin Hu, Yuping Duan, Xudong Wang, and Chuang Dong (2012) " Dissimilar metal joining of aluminum alloy to galvanized steel with Al-Si, Al- Cu, Al-Si-Cu and Zn-Al filler wires", Journal of Materials Processing Technology, pp. 458-464.

[12] Roulin M., J.W. Luster, G.Karadeniz and A. Mortensen (1999) "Strength and Structure of Furnace- Brazed Joints between Aluminum and Stainless Steel", Welding Research Supplement.

[13] Kadhim Naief Kadhim and Ahmed H. (Experimental Study Of Magnetization Effect On Ground Water Properties).Jordan Journal of Civil Engineering, Volume 12, No. 2, 2018

[14] Lin S. B., J.L.Song, C.L. Yang, C.L. Fan, D. W. Zhang (2010) " Brazability of dissimilar metals tungsten inert gas butt welding- brazing between aluminum alloy and stainless steel with Al-Cu filler alloy", Materials and Design, pp. 2637-2642.